Transformations with liquid phase presence in sintering of powder high-speed steel

Movchan A.V.

PhD in Technical Sciences
National metallurgical academy of Ukraine, Ukraine

Bachurin A.P.

PhD in Technical Sciences
National metallurgical academy of Ukraine, Ukraine

Chernoivanenko E.A.

PhD in Technical Sciences
National metallurgical academy of Ukraine, Ukraine

Abstract
The regularities of phase and structural transformations are studied in composition diffusion change within the compacted powder mixture of alloys, in which the alloying elements concentration corresponds to a standard high-speed steel, but carbon content is different. In one component of the mixture, the carbon percentage does not exceed 0.2% while in the other one it is close to the eutectic mixture (~3.8 %). The method of geometrical thermodynamics is applied to determine the diffusion streams at leveling off the carbon concentration in the powder mixture during heating and holding at temperature higher than a melting temperature of the eutecticum. In the paper, we show the dependency regularities of carbide phase transformation while sintering its volume fraction and holding time.
Key words: PHASE TRANSFORMATION, MIXTURE OF POWDERS, HIGH SPEED STEEL, LIQUID-PHASE SINTERING, GEOMETRIC THERMODYNAMICS, STRUCTURE, DIFFUSION, EUTECTICUM, STEFAN PROBLEM, SPHEROIDIZATION, CRYSTALLIZATION

Introduction

The conventional technology for high-speed tool production is based on casting and hot working on the blank. This practice has a number of notable drawbacks, including carbide inhomogeneity and low material utilization [1, 2]. However, the problem to obtain dispersion homogeneous structure can be solved by means of contemporary powder metallurgy, the advantages of which are recognized [3, 4]. The high rate of cooling when spraying molten high-speed steel prevents ledeburite eutectic local zones formation, therefore carbide inhomogeneity in powder high-speed steels is absent. If we compare the results versus those received by the conventional technology, we can find that the dispersion of carbides is 15…20 times better than that of the conventional technology steel (1…2 μm instead of 8…10 μm). The durability of the tool in this case is 1.5…3.5 times higher (it depends on the steel composition and tool dimensions) [5, 6].

The next production process we would like to touch in relation to the topic is ASEA-STORA process, one of the most widely applied production process schemes for blanks of high-speed steel-cutting tool [7, 8]. This scheme incorporates powders compaction by hot gasostatic technique and the subsequent forming. However, the high cost of equipment for hot gasostatic compacting plays in favour of the other scheme to be thought as a more perspective one. The latter includes temper annealing for the sprayed powder, cold compacting in rigid dies and vacuum sintering [9]. Its process permits us to manufacture the blanks, which are maximum close to the geometry of the final tool, and therefore the material utilization ratio is enhanced. Here, there are also opportunities to increase the density in the sintered blanks by means of supersolidus liquid-phase sintering at temperature which is several degrees higher than that of solidus. At this temperature, 4-9% of liquid phase is formed within the structure of the blank under sintering [10]. However, this solution possesses significant drawbacks as follows: the necessity to determine solidus temperature for every chemical composition and to observe strictly the sintering temperature within the narrow range because even a slight overheat above the optimal regime causes a sharp coarsening of the constituents. Regarding all the above mentioned, it could be considered promising to manufacture high-speed steel by the method of compacting and sintering the two powders in which the alloying elements concentrations are as high as those in the standard high-speed steel but the carbon content is different. The carbon concentration in one component mixture is not higher than 0.2%, while in the other one, the carbon content is close to the eutectic (~3.8%). In addition, this technique is based on the researches reported in the earlier papers on phase and structural transformations in diffusion changes within the compositions alloyed as required for high-speed steels [11, 12].

The current paper is devoted to determining the regularities in phase and structural transformations at carbon concentration diffusion leveling off within compacted powder mixture when operations of heating and holding at temperature above eutecticum melting.

Materials and study techniques

The experimental alloys were prepared in the inert atmosphere within the resistance furnace. Their chemical compositions are shown in Table 1.

Table 1. Experimental alloys chemical compositions

	C, %	W, %	Mo, %	Cr, %	V, %	Si, %	Mn, %	Cu, %	S, %	P, %
Alloy I	0.09	6.18	5.26	4.33	1.90	0.17	0.26	0.23	0.013	0.015
Alloy II	3.82	6.45	5.12	4.16	1.84	0.19	0.20	0.10	0.021	0.026

Before feeding, the alloys were mechanically milled as large as 250 μm. The material was compacted at pressure of 600 MPa in capsules made from standard high-speed steel, sealing was applied at this. We obtained compacted alloys density of 95-98% volume ratio, at this the carbon average concentration within the mixture was 1.10…1.12 % wt. The capsules were heated up to the temperature of 1150 °C (the calculated time of through heating was 10 minutes) and held during 30 minutes, 60 minutes and 90 minutes. In order to carry out fixation of the structural state, the samples were quenched in water after completion of their processing. The transformations within these compacts were studied with optical microscopy and geometric thermodynamics.

The results and discussion

The microstructures of the experimental alloys in the initial state are given in Figure 1. Alloy I structure is a coarse grain ferrite with a small number of carbide inclusions of globular form (Figure 1a). The structure of high carbon alloy II is ledeburite eutecticum (Figure 1b). Figure 2 displays the plot of Fe-W-C

diagram at 1150 °C. This diagram is built with the data submitted in [13]. If the tungsten equivalent is taken to stand for the concentrations of the main alloying elements in the alloy, then one can make analysis on the equilibrium in the system under study in the form of approximation ternary diagram and the methods of geometric thermodynamics, including lever rule, could be applied. The dashed line in Figure 2 identifies the chemical composition of alloy I – alloy II diffusion couple within the range from minimal to maximal carbon concentrations. The line passes through several zones of many phases, therefore the diffusion change in the carbon concentration is accompanied by a number of phase and structural transformations. After heating up to 1150°C, the eutectic component of II mixture composition turns into liquid (L) and the process of carbon concentration diffusion leveling off is set off. The generally recognized condition for phase transformations kinetic analysis is thermodynamic equilibrium (equality of component chemical potentials) on phase boundary. At the temperature of sintering, alloy I has a ferrite and carbide structure. If the equilibrium condition is observed then there proceeds the formation of austenite or austenite-carbide layer between the ferrite and carbide constituent and the liquid high-carbon one within the mixture. When carbon concentration is increased in the ferrite and carbide constituent due to the carbon transfer from the high-carbon part through the layer, the disperse carbides (M_6C) are singled out within the ferrite while the initial carbides grow in sizes. If carbon concentration reaches point 1 on ab side, which belongs to α+γ+M_6C triangle, then α-ferrite of composition a, M_6C carbide of composition b, and austenite (γ) of composition c are in the state of equilibrium. The further increase in the carbon concentration causes ferrite decomposition into austenite and M_6C carbide. The carbide is distinguished within the inclusions, which have already been found in the structure (Figure 3a). This corresponds to the results obtained earlier with cementation of low carbon matrix alloys of high-speed types [14, 15].

After austenite layer formation, the melt composition of high-carbon constituent on the boundary with this austenite layer corresponds to point 5 on fh line, which distinguishes zones L and L+γ. The carbon concentration profile at the initial instant of interaction is given in Figure 4a. In order to determine the rate of interphase boundary movements, we apply Stefan problem with the following data:

$$\left(C_5 - C_3\right)v_1 = D_\gamma \left.\frac{\partial C_\gamma}{\partial r}\right|_{r=r1} - D_L \left.\frac{\partial C_L}{\partial r}\right|_{r=r1}, \quad (1)$$

$$\left(C_2 - C_1\right)v_2 = D_\alpha \left.\frac{\partial C_\alpha}{\partial r}\right|_{r=r2} - D_\gamma \left.\frac{\partial C_\gamma}{\partial r}\right|_{r=r2}, \quad (2)$$

where C_n is carbon concentration at an appropriate point or phase; $v_{1,2}$ - rates of interphase boundary movements; D_f – carbon diffusion coefficient in f phase.

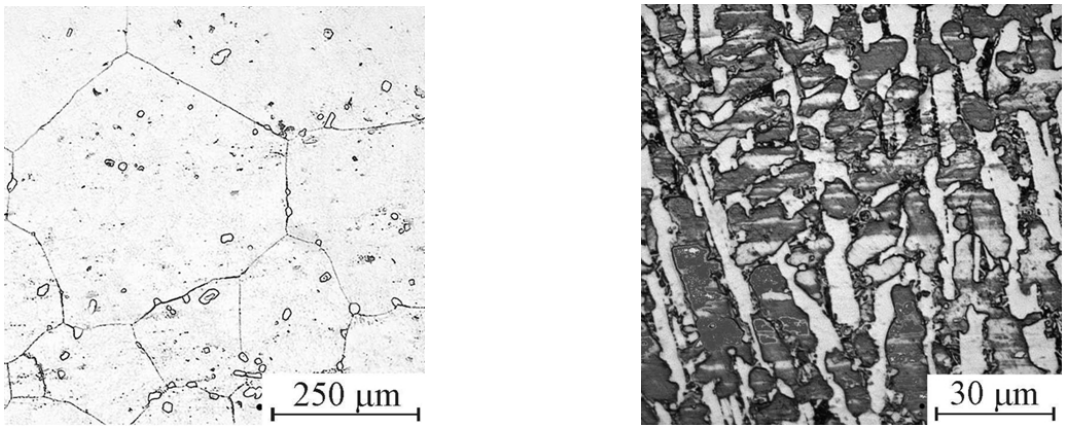

a) b)

Figure 1. Microstructure initial states of the alloys under research:
a – alloy I, b – alloy II

In this case, the Stefan problem does not possess an analytical solution unless significant simplifications. However, without numerical calculations to carry out one can state as follows. Taking into account that $D_\alpha >> D_\gamma$ and convective transfer of the melt, it is thought that crystallization at the initial instant of interaction is impossible because of the intensive delivery of carbon to the interphase boundary. On the contrary, some shift of austenite-carbide layer to the side of low carbon constituent is quite possible along with the amount increase in the liquid phase. The crystallization begins only when the melt composition approaches point 5 and decreases gradient

$$\left.\frac{\partial C_L}{\partial r}\right|_{r=r1}.$$

According to [16], the decarburization of the melt with such composition causes austenite crystallization accompanied with the shift of the alloying elements into melt. The melt is gradually saturated with the alloying elements and reaches f composition (Figure 2). The further decarburization activates the mechanism similar to eutectic, which makes similar crystallization of γ and M_6C phases. The projection of lines separating single-phase L field and two-phase L+γ and L+M_6C field into carbon loss value allows us to determine transverse gradient of main alloying elements concentration in the melt. During crystallization, all these elements are to be distributed completely between γ and M_6C phases. The eutectic morphology is similar to that of the standard high-speed steel in the cast form [16]. However, metallographic analysis performed on the sintered samples showed that there was no pure austenite at the area where the two constituents of the mixture contact. Probably, it was due to a small difference in concentrations in point 5 and point f with short diffusion paths and this resulted in greater gradient carbon concentration; the crystallization process had the fast rate while the austenite crystallization was being suppressed. The carbon distribution within the sintered couple in equilibrium process is reported in Figure 4b.

After completion of crystallization, the further carbon concentration leveling off within the sample volume is described by the following expression:

$$C(r,\tau) = C_{iii} + \sum_{n=1} A_n \frac{\sin\frac{\mu_n}{R} r}{r} \exp\left(-\frac{\mu_n^2}{R^2} D_\gamma \tau\right), \quad (3)$$

where μ_n – are roots of the secular equation $\mu_n = tg\,\mu_n$, obtained from this condition:

$$\left.\frac{\partial C(r,\tau)}{\partial r}\right|_{r=R} = 0 \qquad A_n = \frac{2}{R}\int_0^R rC(r,0)\sin\frac{\mu_n}{R} r dr \quad .$$

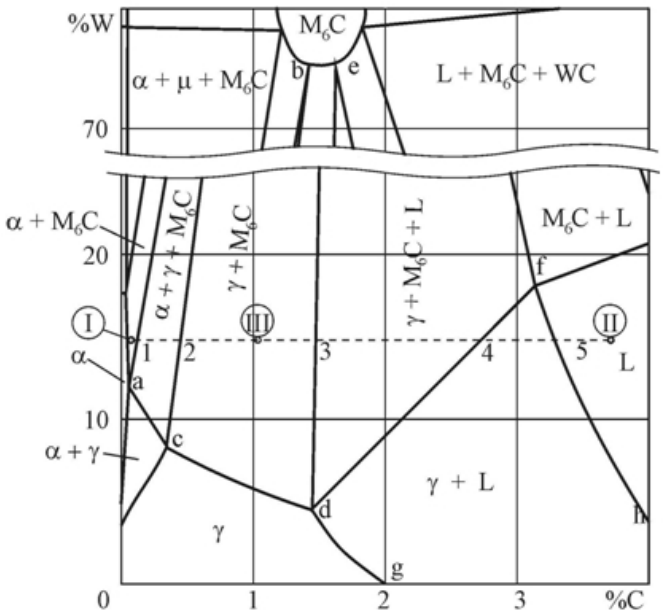

Figure 2. Scheme for a plot of isometric section diagram for Fe-W-C state at 1150 °C

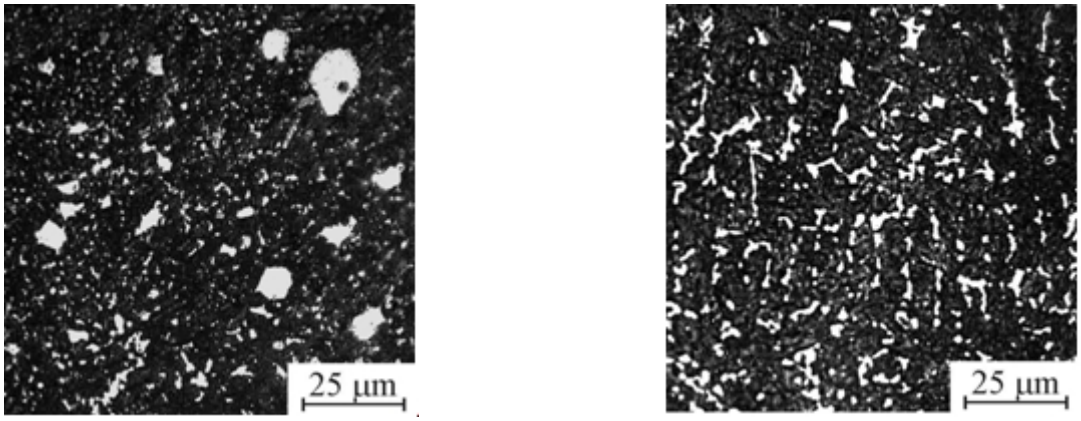

a) b)

Figure 3. Microstructure of the powder mixture under analysis during the sintering process: a – initial state, b – after 30 minutes of sintering

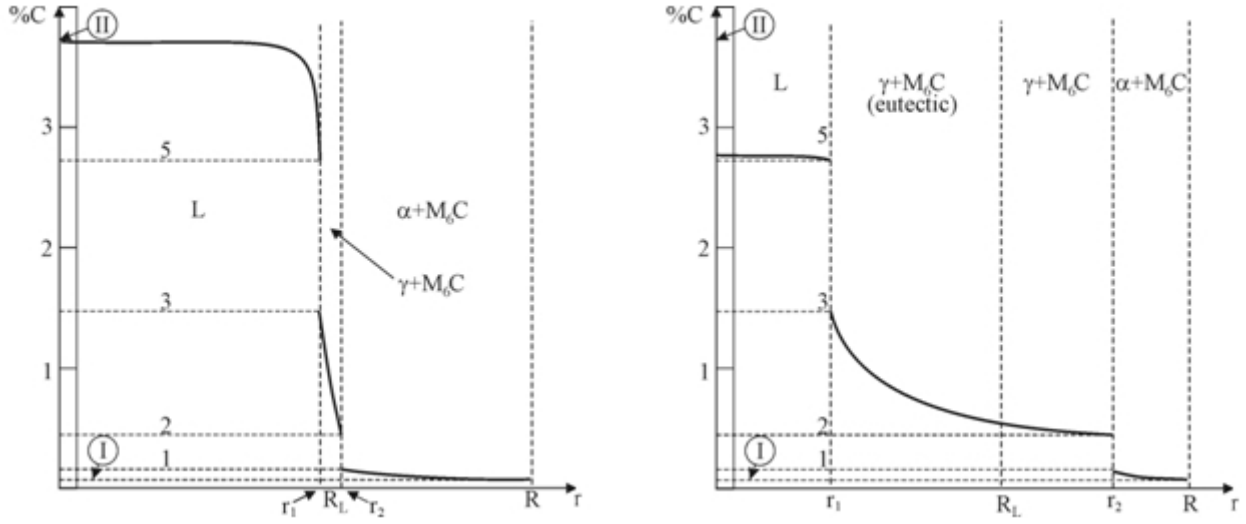

a) b)

Figure 4. Carbon distribution in diffusion couple by means of spherical coordinates for symmetric case. The origin of coordinates is in the melted particle: R_L - radius of the melted particle; R - half a distance between the melted particle and the neighboring one; r_1 – location of L / γ+ M_6C boundary; r_2 – location of γ+ M_6C / α+ M_6C boundary; the digits in the graph correspond to figure 2; a – initial instant of interaction; b – stability stage

Even if C (r, 0) is invariable, nevertheless this expression allows us to assess the time when the maximum amplitude of Fourier expansion decreases down to the value acceptable by the requirements to the appropriate steel grade.

The volume fraction of M_6C carbide with account to the density of 12000-12500 kg/m^3 can be determined by state diagram (Figure 2) with lever rule. At carbon concentration leveling off and resultant decrease from 1.5 to 1.05 (point 3 and point III respectively), the volume fraction of carbide decreases from 0.09 to 0.07. The eutecticum in this alloy has a skeleton morphology that is close to that of rod-like type. The phase morphology in the form of a continuous rod is stable at its volume fraction higher than 0.155 while at lower one the globular morphology shows its stable character. Therefore, the skeleton morphology of eutecticum in alloy II is unstable. One of the methods to simulate transformations of the fibres carbides into globulars (spheroidization) is the method of superposing cosinusoidal perturbations with infinitesimal amplitude (δ) onto the fibre [17]:

$$r(z) = r_0 + \delta \cdot \cos(\omega \cdot z), \quad (4)$$

where r_0 – radius of fibre perturbation;

$\omega = \frac{2\pi}{\lambda}$, λ - length of perturbation wave;

z – coordinate directed along the fibre axis.

Main curvatures of the fibre surface are calculated with the accuracy to the first order with respect to δ and written as:

$$k_1 = \delta\omega^2 \cos(\omega \cdot z), \quad (5)$$

$$k_2 = \frac{1}{r_0} - \frac{\delta}{r_0^2}\cos(\omega \cdot z). \quad (6)$$

Fibre surface curvatures lead to the development of Laplace pressure on the surface and the subsequent shift of the boundary equilibrium concentrations of the alloy components. Directed along the fibre surfaces, the components diffusion flows, which appear during this process, either develop or smooth the superposed perturbations. The perturbation is smoothed if δ and ω are equal at high values of r_0 while at low ones they are developed. The perturbation growth proceeds with the increasing rate and spheroidization completes fast.

Figure 3b illustrates the structure of high-carbon grains after its 30 minute processing. The longer holding did not show any significant structural changes but only accompanied with carbon concentration leveling off in the austenite matrix of the material.

Conclusions

The results reported in this paper permit us to reveal a number of issues of structure formation and phase transformation at sintering with liquid phase carried out for powder mixture of low carbon high-speed steel and high-carbon alloy, produced by technology for high-speed steel alloying. They have not been studied before. Sintering combined with crystallization and spheroidization enables one to obtain the material without inhomogeneity. Moreover, the presence of component with around 70% ferrite in the powder mixture allows us to exclude temper annealing at the stage before compacting from the production scheme. The data received give opportunities to control the final structure of certain articles more profoundly and subsequently to solve the real problems of improvements on production and operational characteristics for powder high-speed cutting tool.

References

1. Geller Yu.A. (1975) *Instrumental'nye stali* [Tool steels]. Moscow: Metallurgiya. 84 p.
2. Revis I.A., Lebedev T.A. (1972) *Struktura and svoystva litogo rezhushchego instrumenta* [Structure and properties of cast cutting tool]. Leningrad: Mashinostroenie. 128 p.
3. Abramov A.A., Samoylenko L.S., Girshov V.L. (2008) Poroshkovye instrumental'nye stali s dispersnoy strukturoy [Powder tool steels with disperse structure]. *Metalloobrabotka* [Metal working]. No.4, p.p.31-35.
4. Ernst I. C., Duh D. (2004) ESP4 and TSP4, a comparison of spray formed with powder metallurgically produced cobalt free high-speed steel of type 6W-5Mo-4V-4Cr. *Journal of materials science*. No.39. p.p. 6831-6834.
5. Poznyak L. A. (1990) Perspektivy primeneniya poroshkovykh bystrorezhushchikh staley. Poroshkovye bystrorezhushchie stali (struktura, svoystva, tekhnologiya proizvodstva instrumenta) [Application perspectives for powder high-speed steel (structure, properties, tool production technology)]. *Naukova dumka* [Scientific thought]. p.p.5-12.
6. Osadchiy A.N., Revyakin S.V., Kiyko G.V. (1981) Proizvodstvo poroshkovoy bystrorezhushchey stali na zavode Dneprospetsstal' [Manufacture of powder high-speed steel at Dneprospetsstal plant]. *Stal'* [Steel]. No.11, p.p.83-84.
7. Hallstom U. (1980) Les aciers rapides frittes ASP. Characteristiques et performance. Mater. Et Techn. No 2-3. p.p. 61-65.
8. Parabina G.I., Revyakin S.V., Marchenko L.N. (1982) Kachestvo poroshkovoy bystrorezhushchey stali, izgotovlennoy na zavode Dneprospetsstal'. [Quality of high-speed steel powders, produced at Dneprospetsstal plant]. *Poluchenie i primenenie raspylennykh metallicheskikh poroshkov* [Manufacture and application of spray formed metallic powders]. p.p.98-100.
9. Shlyapin S.D. (2003) *Sverkhsolidusnoe spekanie poroshkovykh bystrorezhushchikh staley* [Supersolidus sintering of powder high-speed steels]. Moscow: GINFO, MGIU. 212 p.
10. Authorship certificate of the USSR No.1537706, MPK C 22 C 33/02, B 22 F 3/10. Production technique for articles made from powders of high-speed steels. M.M. Uspens'kiy, I.A. Margolin, V.I. Lyukevich. publ. 23.01.1990. Bull. No.3. 2 p.
11. Movchan V.I., Pedan L.G., Ivanica V.I. (1990) Formirovanie napravlennyh austenito-karbidnyh struktur pri nauglerozhivanii slozhnolegirovannyh stalej [Formation of the directed austenite-carbide structures at carburizing complex alloyed steels]. *MiTOM* [Metal science and

thermal treatment of metals]. No 8, p.p. 12-14.
12. Movchan A.V., Gubenko S.I., Bachurin A.P., Chernoivanenko E.A. (2012) Mekhanizm peritektoidopodobnogo prevrashcheniya pri obezuglerozhivanii bystrorezhushchey stali [The mechanism of peritectoid-like transformation at high-speed steel decarburizing]. *Stroitel'stvo, materialovedenie, mashinostroenie: Sb. nauch. Trudov* [Building, material science, machine building: journal of scientific papers]. Bull. 64. p.p. 262-266.
13. Per Gustafson (1987). A Thermodynamic Evaluation of the C-Fe-W System. *Met. Trans*. Vol. 18A. No 2. p.p. 175-188.
14. Vunin K.P., Movchan V.I., Pedan L.G. (1975) Strukturoobrazovanie pri izotermicheskom nauglerozhivanii zheleznykh splavov legirovannykh molibdenom and vol'framom [Structure formation at isothermal carburization of ferrous alloys with molybdenum and tungsten]. *Metally* [Metals]. No.3. p.p.164-168.
15. Movchan V.I., Pedan L.G., Gerasimenko V.P. Movchan V.I., Pedan L.G., Герасименко В.П. (1983) Rost karbidnykh volokon pri diffuzionnom nauglerozhivanii zheleznykh splavov [The growth of carbide fibres at diffusional carburizing for ferrous alloys]. *MiTOM* [Metal science and thermal treatment of metals]. No.9. p.p.19-21.
16. Movchan O.V., Bachurin A.P., Chornoivanenko K.O (2014). Zakonomirnosti fazovikh i strukturnikh peretvoren' pri kristalizatsiї rozplavu Fe-W-C v protsesi znevugletsyuvannya [Regularities in phase and structural transformations during crystallization of Fe-W-C melt in carburization]. Metaloznavstvo i obrobka metaliv [*Metal science and thermal treatment of metals*]. No. 2. p.p.46-50.
17. Cline H. E. (1971) Shape instabilities of eutectic composites at elevated temperatures. *Acta Met*. Vol. 19. No 6, p. p. 481-490.